

Multi-scale probability distributions of solar wind speed fluctuations at 1 AU described by a generalized Tsallis distribution

L. F. Burlaga and A. F.-Viñas

Laboratory for Extraterrestrial Physics, NASA Goddard Space Flight Center, Greenbelt, Maryland, USA

Received 9 June 2004; revised 6 July 2004; accepted 6 August 2004; published 28 August 2004.

[1] The probability distributions of changes in the solar speed observed at 1 AU by ACE during 1999 on scales from 1 hour to 171 days and at a scale of 64 sec can be described by a single distribution function. The function is a simple generalization of the Tsallis q -distribution, a probability distribution that was derived from nonextensive statistical mechanics. The fluctuations in speed are related to (1) intermittent turbulence and shocks on the smallest scales; (2) ejecta, corotating streams, slow flows, interaction regions, etc. on intermediate scales; and (3) systems of interacting flows involving all of these features, on scales greater than the solar rotation period. *INDEX TERMS*: 2111 Interplanetary Physics: Ejecta, driver gases, and magnetic clouds; 2139 Interplanetary Physics: Interplanetary shocks; 2149 Interplanetary Physics: MHD waves and turbulence; 2164 Interplanetary Physics: Solar wind plasma. **Citation**: Burlaga, L. F., and A. F.-Viñas (2004), Multi-scale probability distributions of solar wind speed fluctuations at 1 AU described by a generalized Tsallis distribution, *Geophys. Res. Lett.*, *31*, L16807, doi:10.1029/2004GL020715.

1. Introduction

[2] On the scale of a year, the structure of the solar wind is very complex and the solar boundary conditions needed for multiscale deterministic models are not available. A statistical approach is required in addition to deterministic models in order to describe and explain the structure of solar wind at 1 AU and out to 100 AU during an interval of 1 year [Burlaga, 1975, 1995].

[3] Probability distribution functions (PDFs) have long been used to describe turbulence on small scales [Marsch and Tu, 1997]. Burlaga and Forman [2002] (hereinafter referred to as BF) used PDFs to describe the large-scale fluctuations of speed observed at 1 AU during 1999, close to the period of maximum solar activity. There were many transient flows and shocks during 1999 [Richardson *et al.*, 2000]. BF found that the form of the PDFs varied significantly with scale: highly kurtotic at scales of hours, skewed at small and intermediate (days) scales, and Gaussian at scales greater than the solar rotation period, 27 days.

[4] The purpose of this work is to show that all of the PDFs observed in the solar wind speed fluctuations at 1 AU by Burlaga and Forman on scales from 1 hr to 171 days as well as on a scale of 64 sec can be described by a single distribution function, which is a simple generalization of the Tsallis q -distribution [Tsallis, 1988; Tsallis and Brigatti, 2004].

2. The Distribution Function

[5] A nonextensive (non-additive) entropy $S_q = -\sum (p_i^q - 1)/(1 - q)$ was introduced by Tsallis [1988] to derive a generalization of the Boltzmann-Gibbs statistical mechanics. Here p_i is the probability of the i th microstate, and q is a constant measuring the degree of nonextensivity. By extremizing this entropy subject to two constraints, Tsallis derived the “Tsallis q -distribution function”

$$R_q(x) = A_q [1 + B_q(q-1)x^2]^{1/(1-q)} = A_\kappa [1 + B_\kappa x^2/\kappa]^{-\kappa} \quad (1)$$

where $\kappa \equiv 1/(q-1)$. The function on the right of equation (1) is the traditional (empirical) kappa function, used for many years in space physics, but without any foundation on first principles, to model speed distribution functions of plasma particles [Olbert, 1968; Vasyliunas, 1968; Maksimovic *et al.*, 1997; Leubner, 2002]. The Tsallis entropy generalization extends the traditional Boltzmann-Gibbs thermostatics to physical systems where long-range forces, long-memory effects, and multifractal structure are dominant. The Tsallis distribution is kurtotic for small κ and it tends to a Gaussian (i.e., Maxwellian) in the limit $\kappa \rightarrow \infty$ ($q \rightarrow 1$). A transition from kurtotic to Gaussian PDFs at relatively small and large scales, respectively, was observed by BF. The advantage of considering a Tsallis distribution, rather than other PDFs such as that of Castaing *et al.* [1990], is that the former is based on an entropy principle, can be related to statistical mechanics, and contains the traditional Boltzmann-Gibbs statistical mechanics as a special case of the Tsallis thermostatics. The other PDFs in the literature are based on either mathematical convolutions or specific phenomenological models. This entropy principle was motivated by systems with multifractal structure [Tsallis, 1988]. Since multifractal structure is found in the solar wind [Burlaga, 1995], it is reasonable to consider the application of the Tsallis distribution in the studies of the solar wind.

[6] The Tsallis q -distribution is symmetric and has no skewness, so it cannot model the PDFs observed by BF, which were skewed, except in the Gaussian limit. Therefore, we consider a “generalized Tsallis distribution”, obtained by adding a cubic term to the Tsallis distribution in equation (1), viz.

$$R_{q\tau}(dV\tau) = A_\tau [1 + B_\tau(dV\tau)^2/\kappa + C_\tau(dV\tau)^3]^{-\kappa} \quad (2)$$

Our choice of the form for the cubic term is not unique. Beck [2000] used a skew distribution similar to equation (2) to describe laboratory turbulence, but he included a linear term as well as a cubic term. The cubic term is meaningful

only for $dV\tau$ not too large. Beck gave a physical argument in support of his choice of a skew distribution, but it is not necessarily applicable to the physical processes that we consider. We are not aware of a derivation of a skew PDF from an entropy principle generalizing that of Tsallis, but our results provide a reason to search for such a derivation and generalization.

[7] The parameter B_τ is associated with the standard deviation of the Tsallis distribution and C_τ to the skewness of the distribution function. The sign of C_τ in equation (2) dictates the sense of skewness of the distribution. For large negative (positive) C_τ values the skewness of the distribution is towards positive (negative) $dV\tau$. In order to relate the notation in equation (1) to that used by BF to describe PDFs over a wide range of scales τ , we substituted $dV\tau$ for x and the subscript τ for the subscript κ in the last expression on the RHS of equation (1) to obtain equation (2). The coefficients A_τ , B_τ , and C_τ are functions of τ , as is $\kappa \equiv 1/(q(\tau) - 1)$. Here $dV\tau \equiv dVn(t_i) \equiv V(t_i + \tau) - V(t_i)$ where $V(t_i)$ is the speed measured at hour t_i ($t_i = 1, 2, \dots, 8,759$), and $dV\tau$ is a speed increment at t_i measured at lag τ . In Section 3 we consider $\tau_n \equiv 2^n$ (hours), $n = 0, 1, \dots, 12$, and the corresponding sets of speed increments dVn . The lag τ_n determines the scale of the fluctuations represented by $dVn(t_i)$. Section 4 considers a case for very small scales with $\tau = 64$ sec. The effect of shocks is evident at lags of 64 sec and 1 hour.

3. The Observed PDFs and the Generalized Tsallis Distribution

3.1. Observed PDFs and Their Physical Significance

[8] *Burlaga and Forman* [2002] used 8,759 hour averages of $V(t_i)$ measured by ACE [*McComas et al.*, 1998] at 1 AU during 1999 to compute the PDFs of dVn over a wide range of scales. Following BF, we consider explicitly the PDFs of dVn for 6 representative scales ($n = 0, 2, 4, 6, 9, \text{ and } 11$) corresponding to lags of $\tau_0 = 1$ hour, $\tau_2 = 4$ hour, $\tau_4 = 16$ hours, $\tau_6 = 1.3$ days, $\tau_9 = 21.3$ days, and $\tau_{11} = 85.3$ days, respectively. The scales were chosen to illustrate basic types of solar wind speed fluctuations and the transitions between them. The PDFs for $dVn(t_i)$ measured by BF on these scales are shown on a semi-log scale as histograms of the percentage of counts in bins versus dV by the points in Figure 1. The minimum value of the PDFs, $\approx 10^{-4}$, corresponds to 1 count/bin.

[9] At scale of 1 hour ($n = 0$) (Figure 1a) the fluctuations $dV1$ are typical of intermittent turbulence [*Kolmogorov*, 1962] on small scales in the solar wind [*Burlaga*, 1991]. The PDF is very narrow and falls off steeply on a semilog scale, and the PDF is asymmetric, there being more large values of $|dV1|$ for $dV1 > 0$ than for $dV1 < 0$, as noted by *Burlaga and Ogilvie* [1970] for speed fluctuations at 1 AU during 1967. High points on the tail of the distribution in Figure 1a represent a few large jumps in V associated with shocks, stream interfaces, and some discontinuities with large shear. These features can strongly influence the skewness and kurtosis of the distributions, although there are large uncertainties in these statistics owing to the small number of large speed jumps (see Section 4). The scale of 16 hours (Figure 1c) is in the range of the interaction regions, where the largest positive changes in $dV4$ tend to

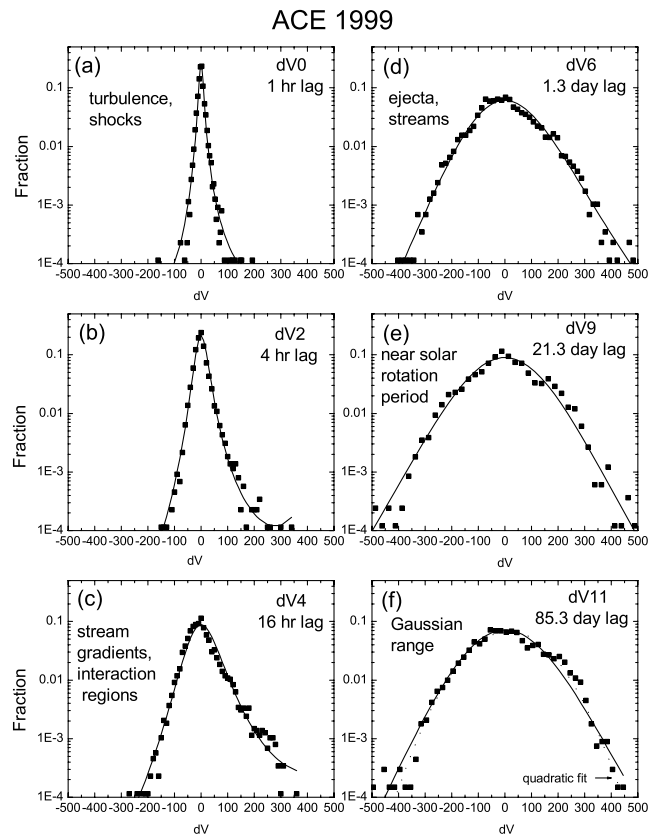


Figure 1. Probability distribution functions of changes of the speed dVn at scales 2^n hours, $n = 0, 2, 4, 6, 9, \text{ and } 11$ observed by ACE (dots) and fitted by the generalized Tsallis distribution function (solid curves). The generalized Tsallis distribution provides good fits to the observed PDFs over the full range of scales considered. At large scales, 85.3 days, the PDF approaches a Gaussian, shown by the dashed curve in panel (f).

occur at the leading edges of streams. As a consequence of stream steepening (faster plasma overtaking slower plasma), there are steeper gradients of V at the front of the streams than at the rear of the streams, giving the observed tail of the PDF and the consequent skewness. The steepening is related to the $\mathbf{V} \cdot (\text{grad } \mathbf{V})$ term in the MHD equation of motion. On a scale of 4 hours (Figure 1b) there is a transition between intermittent turbulence and the changes in V related to the streams. Accordingly, the PDF of $dV2$ has a shape and width intermediate between those of $dV4$ and $dV0$.

[10] The scale of 1.3 days (Figure 1d) is of the same order of magnitude as that of magnetic clouds, complex ejecta, corotating streams, and slow flows (1 to several days), so the fluctuations $dV6$ tend to resemble the flows themselves. The PDF of $dV6$ is broad, and it has an asymmetry (skewness) related to the steepening and expansion of the flows. The scale of 21.3 days (Figure 1e) is close to the solar rotation period (27 days). On this scale one typically observes a mixture of different types of flows and interactions among flows. The PDF is broad, symmetric, and has approximately a Gaussian form (a quadratic on a semi-log scale). On scales larger than the solar rotation period, e.g., the scale of 85.3 days (Figure 1f), one observes a represent-

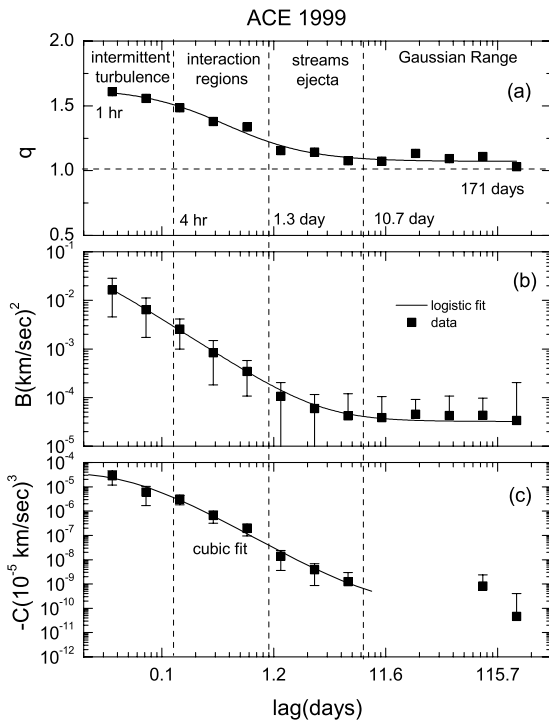


Figure 2. The generalized Tsallis distribution has four parameters A , q , B , C that vary with scale. The values determined by fitting the Tsallis distributions to the observations are shown by the solid squares. Fits of the logistic function to these points for q and B as a function of scale are shown by the curves in (a) and (b). The fit to $-C$ in (c) is a cubic polynomial; in the Gaussian range C fluctuates about 0.

ative sample of the variety of flows characteristic of a particular epoch of the solar cycle activity. On these scales, the PDFs are nearly Gaussian. A fit of the observed PDF of dV_{11} to a Gaussian, shown by the dashed curve in Figure 1f, provides a good fit to the data.

3.2. Fitting the Observed PDFs With the Generalized Tsallis Distribution

[11] We shall now show that all of the different PDFs observed by BF, over the full range of scales from 1 hour to ≥ 85.3 days, can be described by a single function—the generalized Tsallis distribution function, $R_{q\tau}(dV_n)$ given by equation (2). We carried out a weighted non-linear least squares fit to each of the observed PDFs (the points in each of the panels in Figure 1) with $R_{q\tau}(dV_n)$ for $n = 0, 2, 4, 6, 9$, and 11, respectively, using the Levenberg-Marquardt algorithm [Levenberg, 1944; Marquardt, 1963; Bard, 1974]. The results of each of the fits are plotted as the curves in Figures 1a–1f. The theoretical curve provides excellent fits to all of the observed PDFs, from scales of 1 hour to 85.3 days. Non-linear fits of $R_{q\tau}(dV_n)$ to the PDFs for the other values of n , not shown for brevity, are also very good as demonstrated below.

[12] The generalized Tsallis distribution accurately describes the observed PDFs of dV_n over nearly four decades of scales, representing the various types of motions ranging from intermittent turbulent containing shocks and discontinuities on the smallest scales, to various types of

flows (complex ejecta, magnetic clouds, corotating streams, and slow flows) at intermediate scales, and to collections of all of these types of motions at scales of the order of 1 to 3 solar rotations and more.

[13] A fit of $R_{q\tau}(dV_\tau)$ to an observed PDF at scale τ gives a set of parameters: $\kappa(\tau) = 1/(q(\tau) - 1)$, B_τ , C_τ , and a normalization constant A_τ . We computed a fit and this set of parameters for each of the PDFs observed at scales $\tau_n = 2^n$ hours for $n = 0, 1, 2, \dots, 12$. The resulting values of q_n , B_n , and C_n are plotted versus τ_n in Figures 2a, 2b, and 2c, respectively. Each set of values of q_n and B_n versus τ_n was fitted with the logistic function, $y = A2 + (A1 - A2)/(1 + (x/x_0)^p)$ and the resulting curves $q(\tau)$ and $\log(B(\tau))$ are plotted in Figures 2a and 2b, respectively. Each of the curves $q(\tau)$ and $\log(B(\tau))$ provides a good fit to the corresponding values derived from the fits of the observed PDFs to the generalized Tsallis distribution $R_{q\tau}(dV_\tau)$ at the scales τ . Note that $q = 1.68 \pm 0.11$ at a scale of 1 hr (close to the limit $q = 1.5$ discussed by Beck [2001]), and $q = 1.06 \pm 0.03$ at a scale of 171 days approaching the Gaussian limit $q = 1$ of the Tsallis distribution. The curve $\log(-C(\tau))$ in Figure 2c is approximately a cubic polynomial from 1 hour to several days, beyond which C is close to zero. From the fits to the observed PDFs discussed above we calculated moments (the standard deviation, skewness, and kurtosis), and we found that the computed moments versus scale agree with the observed moments versus scale discussed by BF.

4. The Probability Distributions at a Scale of 64 sec

[14] Here we consider whether the generalized Tsallis distribution can also describe the speed fluctuations at a very small scale, $\tau = 64$ sec. Again, we consider the ACE data for 1999, but now we consider 31,575 points (64 sec averages of V). The probability distribution of dV_{64s} is shown by the squares in Figure 3. The lowest points in the PDF correspond to 1 count per bin; although the associated uncertainties are large, the points are significant because

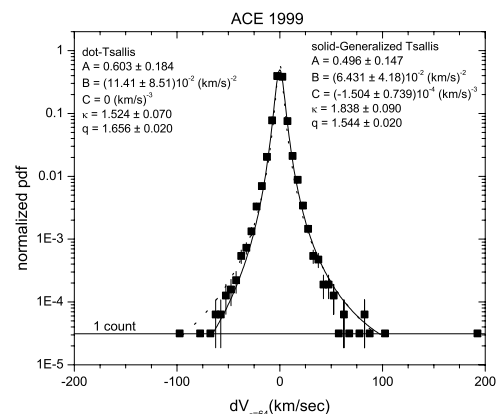


Figure 3. The PDF for very small scale speed fluctuations, at a lag of 64 sec, is shown by the solid squares. The solid curve is a fit of the data points to the generalized Tsallis distribution, and the dashed curve is a fit to the Tsallis distribution.

they represent major structures in the solar wind such as shocks.

[15] The solid curve in Figure 3 is a fit of the generalized Tsallis distribution (equation (2)) to the data. The fit is excellent over 3 decades, and it is consistent with all of the observations within the uncertainties, over more than 4 decades. The dashed curve in Figure 3 is a fit of the Tsallis distribution (equation (1)) to the data. This fit is also excellent over 3 decades, and it too is consistent with all of the observations within the uncertainties. The Tsallis distribution differs from the generalized Tsallis distribution only for small values in the negative wing of the observed PDF. Note that $q = 1.656 \pm 0.070$ for the Tsallis distribution and $q = 1.544 \pm 0.020$ for the generalized Tsallis distribution, close to the limit $q = 1.5$ discussed by Beck [2001]. The results of this section and Section 3 show that the generalized Tsallis distribution describes the observed PDFs on scales from 64 sec to 171 days, the ratio of scales being 203,850, more than 5 orders of magnitude.

5. Summary and Discussion

[16] We have shown that the probability distributions of changes in the solar speed observed at 1 AU during 1999 [Burlaga and Forman, 2002] over nearly four decades of scales, from 1 hour to 171 days (6 solar rotation periods) can be described by a single distribution function with 3 scale-dependent parameters and a normalization constant. One can also describe the PDF of the speed variations during 1999 on a scale of 64 sec by the same function. The function is a simple generalization of the Tsallis q -distribution that was derived from nonextensive statistical mechanics, viz., $R_{q\tau}[dVn(t)] = A_\tau [1 + B_\tau (dVn)^{2/\kappa} + C_\tau (dVn)^3]^{-\kappa}$, which reduces to the Tsallis distribution function when the “skewness coefficient” $C_\tau = 0$. Here $\kappa = 1/(q - 1)$, where q is the nonextensive entropy parameter introduced by Tsallis. The distribution is kurtotic and skewed at small scales where κ is small, and it approaches a Gaussian at large scales in the limit as κ goes to infinity ($q = 1$; $\kappa = \infty$).

[17] The generalized Tsallis distribution describes several types of motions in the solar wind at 1 AU: (1) intermittent turbulence and shocks on the smallest scales; (2) magnetic clouds, complex ejecta, corotating streams, slow flows, interaction regions, etc. on intermediate scales; and (3) systems of interacting flows involving all of these features, on scales greater than the solar rotation period.

[18] The q , B , and C in the generalized Tsallis distribution are functions describing the different types of speed fluctuations in the solar wind on scales from 1 hour to 171 days. We have shown that the curves $q(\tau)$ and $B(\tau)$ derived from the fits of the generalized Tsallis distribution

to the observed PDFs at different scales at 1 AU during 1999 can be described by the logistic function.

[19] **Acknowledgment.** We are grateful to D. McComas for providing the speed data from the SWEPAM instrument on ACE and to Miriam Forman for very helpful comments on a draft of this paper.

References

- Bard, Y. (1974), *Nonlinear Parameter Estimation*, chaps. 4–7, p. 54, Academic, San Diego, Calif.
- Beck, C. (2000), Application of generalized thermostatics to fully developed turbulence, *Physica A*, 277, 115.
- Beck, C. (2001), On the small-scale statistics of Lagrangian turbulence, *Phys. Lett. A*, 287, 240.
- Burlaga, L. F. (1975), Interplanetary streams and their interaction with the earth, *Space Sci. Rev.*, 17, 327.
- Burlaga, L. F. (1991), Intermittent turbulence in the solar wind, *J. Geophys. Res.*, 96, 5847.
- Burlaga, L. F. (1995), *Interplanetary Magnetohydrodynamics*, Oxford Univ. Press, New York.
- Burlaga, L. F., and M. Forman (2002), Large-scale speed fluctuations at 1 AU on scales from 1 hour to 1 year: 1999 and 1995, *J. Geophys. Res.*, 107(A11), 1403, doi:10.1029/2002JA009271.
- Burlaga, L., and K. Ogilvie (1970), Heating of the solar wind, *Astrophys. J.*, 159, 659.
- Castaing, B., Y. Gagne, and E. J. Hopfinger (1990), Velocity probability density functions in high Reynolds number turbulence, *Physica D*, 46, 177.
- Kolmogorov, A. N. (1962), A refinement of previous hypothesis concerning the local structure of turbulence in viscous incompressible fluid at high Reynolds number, *J. Fluid Mech.*, 13, 82.
- Leubner, M. P. (2002), A nonextensive entropy approach to kappa-distributions, *Astrophys. Space Sci.*, 282, 573.
- Levenberg, K. (1944), A method for the solution of certain problems in least squares, *Q. Appl. Math.*, 2, 164.
- Maksimovic, M., V. Pierrard, and P. Riley (1997), Ulysses electron distributions fitted with kappa functions, *Geophys. Res. Lett.*, 24, 1151.
- Marquardt, D. (1963), An algorithm for least-squares estimation of nonlinear parameters, *SIAM J. Appl. Math.*, 11, 431.
- Marsch, E., and C.-Y. Tu (1997), Intermittency, non-Gaussian statistics and fractal scaling of MHD fluctuations in the solar wind, *Nonlinear Processes Geophys.*, 4, 101.
- McComas, D. J., et al. (1998), Solar wind electron proton alpha monitor (SWEPAM) for the Advanced Composition Explorer, *Space Sci. Rev.*, 86, 563.
- Olbert, S. (1968), Summary of experimental results from M.I.T. detector on IMP-1, in *Physics of the Magnetosphere*, edited by R. L. Carovillano, J. F. McClay, and H. R. Radoski, p. 641, Springer-Verlag, New York.
- Richardson, I. G., D. Berdichevsky, M. D. Desch, and C. J. Farrugia (2000), Solar-cycle variation of low density solar wind during more than three solar cycles, *Geophys. Res. Lett.*, 27, 3761.
- Tsallis, C. J. (1988), Possible generalization of Boltzmann-Gibbs statistics, *J. Stat. Phys.*, 52, 479.
- Tsallis, C., and E. Brigatti (2004), Nonextensive statistical mechanics: A brief introduction, *Continuum Mech. Thermodyn.*, 16, 223.
- Vasyliunas, V. M. (1968), A survey of low-energy electrons in the evening sector of the magnetosphere with OGO 1 and OGO 3, *J. Geophys. Res.*, 73, 2839.
- L. F. Burlaga and A. F.-Viñas, Laboratory for Extraterrestrial Physics, NASA Goddard Space Flight Center, Mail Code 692, Bldg. 21, Rm. 244, Greenbelt, MD 20771, USA. (leonard.f.burlaga@nasa.gov)